

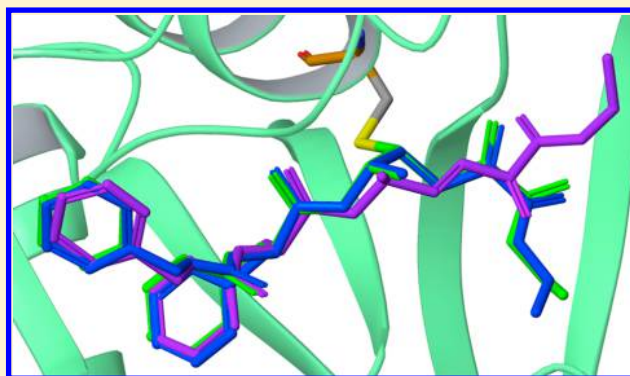
Docking Covalent Inhibitors: A Parameter Free Approach To Pose Prediction and Scoring

Kai Zhu,[‡] Kenneth W. Borrelli,[‡] Jeremy R. Greenwood, Tyler Day, Robert Abel, Ramy S. Farid, and Edward Harder*

Schrodinger Inc., 120 West 45th Street, New York, New York 10036, United States

S Supporting Information

ABSTRACT: Although many popular docking programs include a facility to account for covalent ligands, large-scale systematic docking validation studies of covalent inhibitors have been sparse. In this paper, we present the development and validation of a novel approach for docking and scoring covalent inhibitors, which consists of conventional noncovalent docking, heuristic formation of the covalent attachment point, and structural refinement of the protein–ligand complex. This approach combines the strengths of the docking program Glide and the protein structure modeling program Prime and does not require any parameter fitting for the study of additional covalent reaction types. We first test this method by predicting the native binding geometry of 38 covalently bound complexes. The average RMSD of the predicted poses is 1.52 Å, and 76% of test set inhibitors have an RMSD of less than 2.0 Å. In addition, the apparent affinity score constructed herein is tested on a virtual screening study and the characterization of the SAR properties of two different series of congeneric compounds with satisfactory success.



1. INTRODUCTION

Covalent drugs are a unique class of drugs, which form a covalent bond with their target protein. They derive their activity not only from noncovalent interactions but also from the formation of the covalent bond between the inhibitor and the target protein. Mostly due to safety concerns regarding possible off-target reactivity liabilities, covalent drugs have been disfavored and underdeveloped as a drug class.¹ However, there has been a resurgence of covalent drug research in recent years, with the HCV protease inhibitors telaprevir² and boceprevir³ representing two prominent examples. It has been realized that covalent drugs may offer unique opportunities in drug design campaigns. For example, the warhead of a covalent inhibitor might be used to target a rare, nonconserved residue across a protein family amenable to such reactive targeting and thus achieve highly selective inhibition against the desired target versus most other members of the protein target family.⁴ For shallow binding pockets, the covalent inhibition approach might also be utilized to provide additional binding potency that could be highly challenging to obtain through noncovalent interactions.^{2,3,5} To ameliorate safety concerns, the off-target reactivity can be minimized by designing inhibitors with binding modes that require a specific combination of noncovalent and covalent interactions, thus creating the potential for molecules that provide a binding specificity comparable to that provided by traditional highly optimized noncovalent inhibitors.

Computational docking has become an integral part of structure based drug design, but the majority of docking methods development research has been focused on the effective prediction of the binding modes of noncovalent inhibitors.^{6–8} Popular docking programs often include a facility to dock and score covalent inhibitors by way of a variety of different approaches. For example, GOLD⁸ defines a “link atom” both in the ligand and in the protein and forces the ligand link atom to occupy the same steric volume as the protein link atom to mimic the covalent binding event. Autodock⁷ offers two methods to dock the covalently bound ligands: (1) a grid-based approach employs a Gaussian biasing function centered on the protein attachment atom and also the grid-based energy to bias the covalent bonding ligand pose; (2) a flexible side chain approach treats the covalently bound ligand and the protein attachment side chain as a single flexible side chain and samples it as part of the receptor. However, these methods have generally only been demonstrated with anecdotal case studies,^{8,9} and large-scale and systematic validations have been sparse. To our knowledge, the only systematic study with substantial data set in the literature is CovalentDock by Ouyang et al.¹⁰ Their work uses a dummy atom to force covalent bond formation and scores the contribution of the covalent bond with a Morse potential parametrized for the specific chemical

Received: February 24, 2014

Published: June 11, 2014

reaction of interest. They have tested their approach with the pose prediction of 76 covalently bound complexes and a virtual screening study.

In this paper, we present an approach for docking and scoring covalent inhibitors that consists of conventional noncovalent docking of the prereactive species, heuristic formation of the covalent attachment, and structural refinement of the covalently bound protein–ligand complex. We utilize the rapid sampling provided by the docking program Glide^{6,11,12} to generate a large pool of initial poses for the prereactive species. Then, based on geometric criteria, a subset of poses are selected and covalently linked to the receptor. The protein structure prediction and refinement program Prime^{13–18} is then used to simultaneously optimize the ligand pose and the attachment residue to produce a sound physical geometry. The resultant protein–ligand complex geometries are ranked based on VSGB2.0, an all-atom energy function based on OPLS force field and Generalized Born solvation model,¹⁸ which has been extensively validated in the context of protein structure prediction. The covalent bond parameters are taken from the OPLS force field, such that any nonphysical bond distances, angles, or torsions will be appropriately penalized. This strategy eliminates the need to develop new parameters for new chemical reaction types, which makes this approach naturally extendable to many additional reaction types that may be of interest to the medicinal chemistry project team. To estimate the SAR properties of the series, we have developed a scoring procedure that utilizes information from both the Glide scores of the unbound prereactive species and the Glide score of the covalently bound final predicted binding mode. This scoring function does not model the bond formation energy directly, but it captures the fitness of the covalent bond implicitly. In particular, this scoring procedure amounts to assuming a promising covalent inhibitor must bind with high affinity prior to reacting to form a covalent bond with the protein and must not form especially energetically unfavorable contacts with the protein after the reaction has completed, or else the formation of such energetically disfavored contacts would disfavor the formation of the covalent bond. We expect such an approximation to be reasonable when the intrinsic reactivity of the reactive warhead of the inhibitors of the series is largely unmodified across the series but will be quite poor if the intrinsic reactivity of the reactive warhead is being aggressively tuned, in which case a more thorough treatment of the associated issues may require a detailed quantum mechanical investigation to be more properly handled.

We have extensively tested the above method by attempting to reproduce the binding geometry of 38 covalently bound protein–ligand complexes. Its performance on pose prediction is also compared with CovalentDock head-to-head on the same set of 76 complexes reported in the original CovalentDock reporting publication. In addition, we have also tested the ability of the method to enrich the active compounds from a library of decoy compounds and rank-order two series of congeneric covalent inhibitors vs their measured activities.

2. MATERIALS AND METHODS

2.1. The Workflow. Our approach to covalent docking is designed to mimic key steps in the binding pathway. A successful covalent inhibitor in its prereactive form must first be able to fit in the binding site with a pose that brings the respective reactive groups of the ligand and receptor into close proximity. Noncovalent interactions must be able to maintain

an appropriate stable binding mode for a sufficiently long time to allow for the covalent bond to form. The receptor and ligand may undergo conformational changes to facilitate the covalent reaction, but throughout the reaction process, the noncovalent interactions must keep the ligand appropriately positioned in the binding site for the reaction to proceed. Finally, the geometry of the ligand and receptor residue should exert minimal strain on the covalent bond and ligand pose in the binding site in the postreactive form. These different stages are reflected in the stages of the workflow discussed below and illustrated in Figure 1.

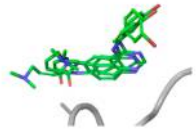
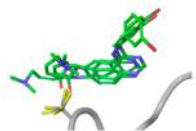
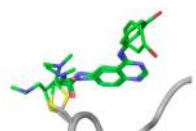
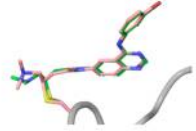
Protocol		Number of Poses
Docking of the pre-reactive species of the ligand into the Alanine mutated form of the receptor		20-100
Mutation of the attachment residue back to its original chemical structure, and sampling rotamer states of that residue consistent with covalent bond formation		120-600
Reaction of the ligand with the receptor to form the covalent complex.		60-300
Clustering the resulting poses and optimization of the covalent complex		30-50
Selection of the optimal structure(s) as per Prime energy ranking		1

Figure 1. Workflow of the covalent docking protocol using Glide and Prime.

Step1: Noncovalent Docking. To ensure exhaustive conformational sampling ConfGen¹⁹ is used at the outset to sample ligand conformations and select 3 low energy conformations for Glide docking. To avoid clashes with the protein and to minimize conformational bias, the reactive residue is mutated to alanine before the docking stage. A positional constraint in Glide is applied to keep the ligand reactive moiety within 8 Å of the C-beta atom of the receptor reactive residue. All ligand poses with a Glide score within 2.5 kcal/mol of the lowest sampled score are retained.

Step2: Receptor Sampling. The reactive residue is then mutated back to the original amino acid and its side chain conformation is sampled with a rotamer library. Each sampled binding mode is checked to see if the two atoms that will ultimately form the covalent bond between the ligand and target are within 5 Å of each other. Any pose that does not satisfy this criterion is discarded. While this distance is much longer than would be physically realistic, downstream optimization steps will correct or eliminate any poses that would not allow the bond to be formed.

Step3: Covalent Bond Formation. The covalent bond is then formed along with any bond order changes, protonation changes, etc. that occur upon formation of the covalent bond. If

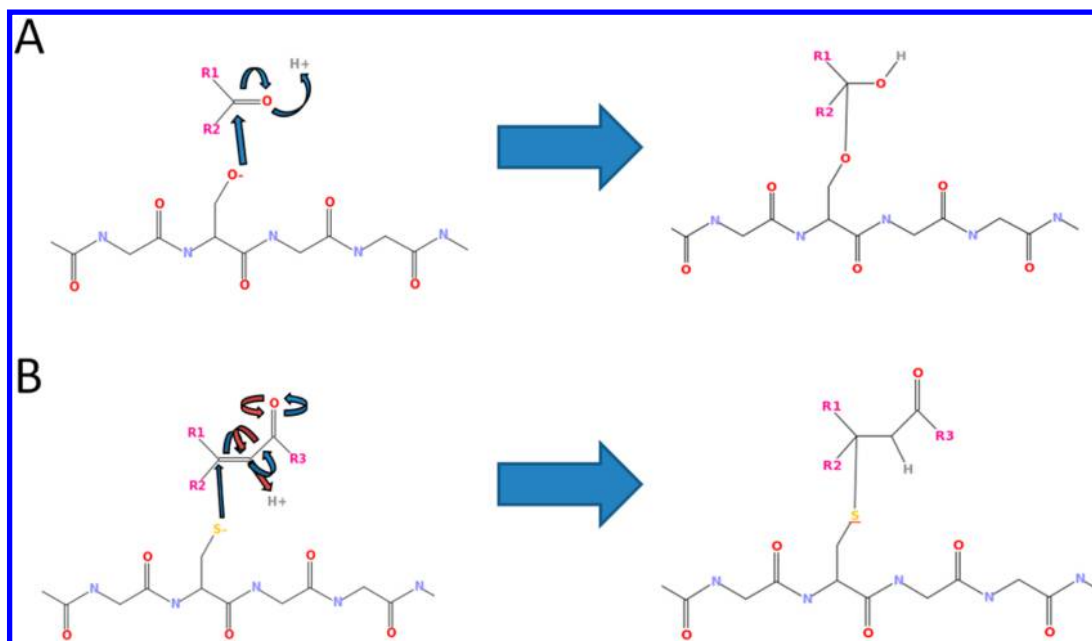


Figure 2. Electron pushing scheme for the Nucleophilic addition (Panel A) and the two-step Michael addition (Panel B). The first step of the reaction is shown in blue arrows and the second step (for Michael addition) in red arrows. Note in both reactions that the change in hybridization from sp^2 to sp^3 of the carbon attached to functional groups R1 and R2 can drastically affect the relative orientations of the three functional groups (R1, R2, and R3) when the functional groups are either large or connected to each other by a ring.

the reaction can lead to different chiral centers, then all stereoisomers are retained for further structural optimization.

Step4: Refinement. The covalent complexes are then minimized in vacuum to restore normal bond lengths and resolve steric clashes. These partially optimized poses are then clustered by their Cartesian coordinates using a k-means algorithm. This step both produces a reasonable starting point for further optimization and eliminates duplicate poses. The selected poses, including the ligand and the bonded receptor residue, are then minimized using the Prime VSGB2.0 energy model.¹⁸ The final Prime energy subsequent to minimization of the covalently bound complex is then finally used to rank the poses and select the most likely binding geometry.

Step5: Apparent Affinity Scoring. To rank compounds we have developed an empirical scoring function that estimates the apparent affinity of a covalent inhibitor without including a direct calculation of the bond formation energy. Our apparent binding affinity score is defined as the averaged Glide score taken at two steps in the simulated reaction process: the first is the Glide score of the binding mode of the prereactive ligand species, and the second is the approximate Glide score of the ligand in the covalent complex after formation of the covalent bond. This combined score captures the essential elements during a covalent docking process. First, a covalent binder in its prereactive form must be able to occupy the binding pocket with appreciable residency time to facilitate reaction of the covalent inhibitor warhead with the target protein residue. Second, as the reaction proceeds, unfavorable steric clashes or poor electrostatic contacts should not be formed in the covalent complex, or else these unfavorable contacts will oppose the reaction running to completion. Thus, an optimal covalent inhibitor should have favorable noncovalent interactions with the protein target of interest before and after reaction and therefore a low Glide score in both steps. The full workflow is diagrammatically depicted in Figure 1. Figure 2 as an example depicts a reaction diagram of two chemical reactions

(Nucleophilic addition and Michael addition) analyzed in this work. The entire process has been automated for both the reactions presented here and for several other reaction types. Additional types of reaction are also supported in the workflow.

A typical covalent docking prediction with this method takes 1–3 CPU-hours per ligand to complete. The workflow can be easily customized for different requirements in terms of balancing the speed and accuracy. For example, we can increase the amount of sampling and pose optimization to accurately score systems with large conformational changes that occur upon covalent bond formation or reduce the amount sampling to create protocols amenable to higher-throughput screening.

2.2. System Preparation. As input, the procedure accepts ligands prepared in their prereactive form. Ligands are prepared with LigPrep²⁰ in Maestro v9.5,²¹ and Epik^{22,23} is used to generate different tautomer states. If multiple tautomer states are accessible, then the tautomer with the lowest Epic ionization penalty is chosen. The receptor protein is prepared with the Protein Preparation Wizard.²⁰

2.3. Data Sets. We have tested our covalent docking protocol, hereinafter referred to as CovDock, with data sets aimed at addressing three common applications of docking in the context of the discovery of therapeutically valuable covalent inhibitors: pose prediction, virtual screening, and SAR characterization.

The first test involves assessing the prediction of the binding mode of the covalent inhibitor. We here collected 38 complexes from the PDB database covering two common reaction types: 27 cases involve Michael addition and 11 are Nucleophilic addition. All of them are experimentally observed, as expected, to exhibit a covalent bond between the ligand and the receptor. If the PDB structure was a dimer or multimer, we used the chain with better structure quality, for example, with fewer missing atoms or chain breaks. If both chains were identical, we simply used chain A as the default choice. The list of PDB IDs, chain names, and reactive residue numbers for the full data set

Table 1. Self-Docking Pose Prediction for 38 Crystal Structure Complexes^a

PDB ID	reaction type	reactive residue	Glide prediction	RMSD of the predicted pose (Å)	best RMSD of top 10 poses (Å)	protein family
1u9q	Michael	X:25	2.17	0.97	0.93	Cruzain
2oz2	Michael	A:25	1.06	1.13	1.13	
3lxs	Michael	A:25	1.28	1.26	1.26	
2awz	Michael	A:366	4.81	2.94	2.84	HCV
2ax0	Michael	A:366	4.99	2.14	1.81	NSSB
2ax1	Michael	A:366	4.65	6.19	2.73	polymerase
2c1e	Michael	A:163	2.41	2.78	2.19	caspase-3
2c2m	Michael	A:163	2.05	2.19	1.48	
2c2o	Michael	A:163	2.37	2.14	2.12	ERK2
2c2z	Michael	A:360	3.77	1.17	1.03	
2e14	Michael	A:166	1.11	1.07	1.00	
3c9w	Michael	A:164	0.66	0.52	0.16	cSrc kinase
2hwo	Michael	A:345	4.96	4.95	4.87	
2hwp	Michael	A:345	2.86	2.74	2.06	
2qlq	Michael	B:345	2.51	1.96	1.24	EGFR kinase
2qq7	Michael	A:345	1.73	0.70	0.70	
3lok	Michael	B:345	0.36	1.22	0.39	
3svv	Michael	A:338	0.99	0.17	0.17	aP2
2j5e	Michael	A:797	1.08	0.95	0.35	
2j5f	Michael	A:797	1.22	1.02	0.93	
2jiv	Michael	A:797	1.63	0.94	0.94	BTK
3ika	Michael	A:797	1.03	0.89	0.89	
3js1	Michael	A:117	3.88	1.84	1.51	
3t9t	Michael	A:442	1.62	0.69	0.69	JNK
3v6r	Michael	A:154	2.12	1.12	1.02	HCV NS3/4A protease
3v6s	Michael	A:154	1.72	1.87	1.13	
3oyp	Michael	A:159	0.99	0.46	0.41	
2gvf	Nucleo	A:139	1.12	0.85	0.33	
2obo	Nucleo	A:139	1.42	0.74	0.19	
2oc1	Nucleo	A:139	1.28	0.82	0.40	
2p59	Nucleo	B:1165	1.88	0.95	0.61	
3lox	Nucleo	A:139	1.45	0.73	0.27	
2oc7	Nucleo	A:139	1.50	0.24	0.23	
2oc8	Nucleo	A:139	1.48	0.77	0.27	
2oc0	Nucleo	A:139	1.39	0.75	0.17	
3knx	Nucleo	A:139	1.59	1.38	1.27	
1w3c	Nucleo	B:139	3.48	3.48	1.72	
2f9u	Nucleo	A:139	1.72	0.92	0.45	
% <2 Å			63%	76%	84%	
mean			2.06	1.52	1.10	

^a27 of the structures were formed by Michael addition and 11 were formed by Nucleophilic addition reactions. The prediction accuracy is measured by the ligand heavy atom RMSD (Å).

can be found in Table 1. Further, as an additional validation of the protocol's ability to properly identify the correct binding modes of typical covalent inhibitors, we have also tested against the same data set used by Ouyang et al. as in Table 2 and Supporting Information Table S1.¹⁰

The second test is a virtual screening study, in which our protocol is tested to distinguish covalent inhibitors from a database of putative nonbinders. We used all 12 acrylamide

Table 2. Summary of Pose Prediction Results on the 76 Complexes in CovalentDock^a

	Schrödinger CovDock	CovalentDock	Autodock	GOLD
top 1 pose	1.8	3.4	3.5	4.0
best in top 10	1.4	1.9	2.5	3.4

^aThe accuracy is measured by heavy atom RMSD (Å).

Michael acceptors in our pose prediction data set to mine Schrodinger internal database (CACDB 2011, which had 6 million purchasable compounds) for acrylamide containing compounds and chose the best 100 matches based on fingerprint Tanimoto similarity and property space. The PDB binders were prepared as linear fingerprints using the default atom types. The top 10 fingerprint hits for each ligand probe were pooled into a unique set of 44 compounds. The remaining 57 compounds were selected by a property space proximity technique using MW (molecular weight), MR (molar refractivity), AlogP (lipophilicity of a molecule expressed as log), RB (rotatable bond), HBD (hydrogen bond donor), HBA (hydrogen bond acceptor), PSA (polar surface area), and NH (number of heavy atom) descriptors. Two native ligands in the pose prediction data set, 3t9t and 3oyp, did not recover any meaningful similarity hits (<0.09). Thus, a final set of 10 acrylamide Michael acceptors from the pose prediction data set

was selected as the true binders. The PDB IDs and protein targets of this set of inhibitors can be found in Table 3 and

Table 3. Protein Targets of Active Ligands and Groups of Decoys Used in Virtual Screening Study^a

target	known ligands	number of decoys
cSrc	5	20
EGFR	4	60
JNK	1	20
total	10	100

^aAll known ligands are considered to be active for all three targets.

Table 4. It should be noted that some of the decoys might actually be active molecules, though the likelihood is presumed to be quite low. Both the active binders and decoys were prepared from SMILES with LigPrep,²⁰ and the lowest state penalty variant was selected for the decoy set.

In the third test, our protocol was used to retrospectively rank order two congeneric series of compounds and study the implied structure activity relationships (SAR). These two series covered the two reaction types studied in this work, and their binding pockets had highly distinctive features. The first series included 11 acrylamide inhibitors of cSrc kinase, which undergo a Michael addition with the cysteine residue in the binding pocket. The second series included 26 peptidyle ketoamides which inhibit the HCV serine protease by way of a Nucleophilic addition to the serine residue. The experimental apparent activity IC₅₀ values for these inhibitors are curated from the literature and converted to an apparent binding affinity at 298 K to be compared with our affinity score; the receptor structures and the compounds are prepared the same way as in the virtual screening study.

3. RESULTS AND DISCUSSION

3.1. Pose Prediction. The pose prediction accuracy assessment was based on the heavy atom RMSD between the lowest energy ligand pose and the reference crystal structure. A successful prediction was here defined as within 2 Å of the X-ray structure. The results in Table 1 show that CovDock predicts the experimentally observed pose correctly in 76% of cases and yields an average RMSD of 1.52 Å over the whole set. Expanding the criteria used to select a predicted pose to include any one of the 10 lowest energy poses leads to an increase in accuracy of 84% and 1.10 Å, respectively. Table 1 also includes

structural predictions based solely on the initial Glide docking stage of the CovDock workflow where poses are ranked based on their Glide score. The top ranked success rate and average RMSD are 63% and 2.06 Å, respectively. The drop in accuracy relative to CovDock reflects the additional accuracy provided by the latter Prime refinement stage of the workflow. As an example, Figure 3 contrasts the predicted pose of 1u9q when using the full CovDock workflow (0.97 Å) and just initial Glide docking (2.17 Å).

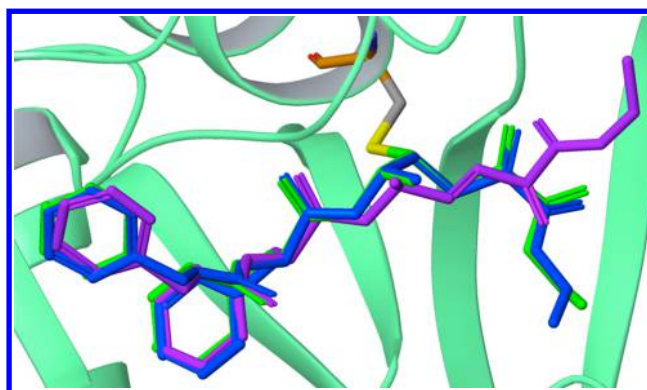


Figure 3. Predicted binding mode of 1u9q is here depicted. In green tube representation is the binding mode observed in the crystal structure, in the purple tube representation is the top scoring pose by Glide score sampled during the initial docking stage (2.17 Å), and in the blue representation is the final prediction determined by Prime energy (0.97 Å).

By protein family, the largest prediction errors fall in the group of HCV NS5B polymerase structures (2ax0, 2ax1, and 2awz). The respective ligands share some common features: an exocyclic rhodanine warhead situated in the center of an extensively conjugated planar system when the ligands are in their prereactive form (see Figure 4). The reaction associated with the covalent inhibition event breaks the π -conjugated link between the rhodanine and (halo)phenyl rings, in turn leading to a large ligand conformational change upon binding. Such molecules present a considerable challenge for the present protocol. Since the prereactive and postreactive forms favor highly dissimilar conformations, the Glide docking stage alone cannot infer the correct postreactive binding mode solely from a sampling of possible binding modes of the prereactive form of the molecule. As shown in Figure 4, the predicted incorrect

Table 4. Distinguishing Binders from Nonbinders^a

PDB ID	target	use Glide score on prereacted pose			use Glide score on postreacted pose			use average Glide score		
		rank of native ligand	active ligands in top 20%	AUC	rank of native ligand	active ligands in top 20%	AUC	rank of native ligand	active ligands in top 20%	AUC
2hwo	cSrc	48	3	0.677	47	2	0.626	36	3	0.780
2hwp	cSrc	4	7	0.804	3	7	0.873	2	7	0.858
2qlq	cSrc	3	8	0.802	11	8	0.835	8	8	0.825
2qq7	cSrc	47	5	0.732	9	7	0.824	13	8	0.836
3lok	cSrc	7	10	0.956	6	8	0.816	5	8	0.864
2j5e	EGFR	3	7	0.862	5	9	0.955	2	9	0.950
2j5f	EGFR	24	6	0.764	7	7	0.842	9	7	0.829
2jiv	EGFR	1	9	0.942	1	9	0.906	1	9	0.941
3ika	EGFR	5	4	0.614	3	5	0.735	3	5	0.701
3v6s	JNK	1	4	0.448	1	3	0.395	1	3	0.428

^aAUC represents for the area under curve for ROC.

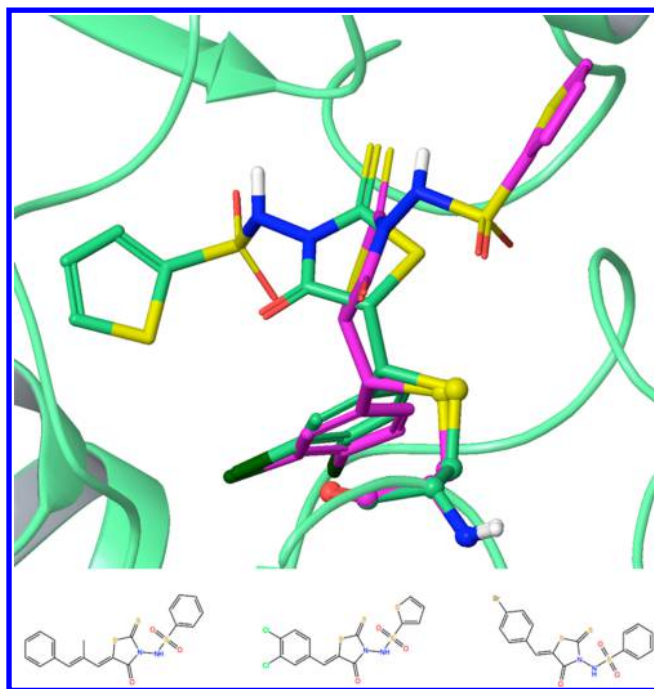


Figure 4. Binding mode prediction of covalent inhibitor 2ax1 is here depicted. The binding mode of the complex observed in the crystal structure is shown in a green tube representation for the protein and a green-carbon-atom representation for the ligand. The predicted binding mode is shown using a purple-carbon-atom representation (RMSD 6.19 Å). The ligand is covalently bound to residue A:366_Cys. The bottom subpanel of the figure shows the chemical structures of the three studied ligands from HCV NSSB polymerase crystal structures 2ax0, 2ax1, and 2awz (from left to right).

pose is in an extended conformation, which shows the significant residual memory of the binding mode of the prereactive form, which must be quite extended due to the conjugated character of the prereactive species. In contrast, the crystal structure the covalent inhibitor displays a binding mode that is much more spatially compact and could not be occupied by the prereactive species. This issue might be addressed by sampling the ligand conformations in both pre- and postreacted form for the Glide docking and is under active investigation.

Ouyang et al.¹⁰ recently described a covalent docking methodology based on Autodock. The authors validate the pose prediction quality of their method using a data set of 76 complexes, out of which 13 involve Michael addition and 63 involve acylation by β -lactam ring-opening. To facilitate a head-to-head comparison, we have assessed the prediction accuracy of our method on the same data set. The average RMSD of our predictions is 1.8 Å. If the best RMSD of the top 10 poses is chosen as the accuracy metric, the average would be 1.4 Å. In comparison, CovalentDock by Ouyang et al. has the RMSD of 3.4 and 1.9 Å for the best of top 1 and top 10 ranked poses, respectively. A summary of the comparison of our results with CovalentDock, Autodock, and GOLD is presented in Table 2. The detailed target lists and results for the 76 complexes are in the Supporting Information Table S1.

3.2. Virtual Screening. The development of the apparent binding affinity scoring function is predicated on an ad hoc assumption regarding the kinetic mechanism of covalent inhibition. Namely, it presumes that the rate of the covalent reaction is sufficiently slow that favorable noncovalent interactions are required to stabilize the prereactive binding

mode and those transient binding modes associated with intermediate stages of the reaction. We take the combination of the pre- and postreactive binding modes of the ligand as a proxy for these states and compute the average Glide score as our measure of apparent binding affinity. Because Glide can only directly score noncovalent ligands, we need to delete the covalent bond between the ligand and the receptor and also mutate the reactive residue to alanine in order to obtain a pseudo-Glide score for the postreactive binding mode. This empirical scoring procedure does not include a component that directly accounts for the formation energy of the covalent bond and thus should not be expected to rank order covalent inhibitors well that differ greatly in their intrinsic reactivities.

To test the validity of the above scoring function, we have designed a virtual screening study based upon a subset of known binders from the pose prediction test set. In total, 10 acrylamide type Michael acceptors were chosen spanning 3 protein targets. Further, given the similarity of the respective binding sites, we assume all 10 ligands bind to all three targets. Note, some of these ligands are known binders of more than one protein in this set. An example is the ligand bound to cSrc (2hwo) and EGFR (2j5e). All receptors have a cysteine as the attachment residue. Then, 100 decoys were selected based on chemical similarity to these known binders using the procedure outlined in Methods. It is understood that some of the decoys may actually be active molecules, and our choice of using only high similarity decoys makes the virtual screening test even yet more challenging than typical virtual screening applications. The chemical structures of the 10 active ligands and 100 decoys are listed in the Supporting Information Table S2. Table 4 shows the ranking of the actives in the total list 110 active and decoy compounds, as well as the number of active compounds in top 20% of selected compounds. Three scoring schemes are compared in Table 4: the Glide score on the prereactive binding mode, the Glide score on the postreactive binding mode, and the affinity score constructed in this work which averages the Glide score of the pre- and postreactive binding modes. Table 4 shows that the average score offers the best and most stable performance among the three scoring schemes. As the results show, the active covalent inhibitors rank very high for all receptors except 2hwo. When the cocrystallized ligand does not rank as the number one ligand, it is most often outranked by other presumed active ligands. The AUC (area under the Receiver Operative Characteristics, ROC) ranges from 0.70 to 0.95 for cSrc and EGFR receptors. The JNK receptor 3v6s is an exception with the AUC of 0.43. As an example, Figure 5 shows one of the best ROC curves with 2jiv as the receptor.

The choice of receptor structure can have a significant effect on the virtual screening. In Table 4, we ran the virtual screening experiments on all 10 PDB structures where the true binders came from. The results had substantial variations across different receptors in terms of active binder ranking and AUC, with two obvious outliers 2hwo and 3v6s. For the relatively poor performance of 2hwo among cSrc group, it might be related to the fact that its loop region near the binding pocket is not well resolved in the crystal structure with multiple residues missing, e.g. A:275, A:407-A:424, etc. On the other hand, using the structure with rebuilt missing residues and loops did not produce improved virtual screening results in our test. There are many factors that go into the docking and scoring process, so it is very hard to pinpoint exactly what is responsible for the failures. For JNK receptor 3v6s, being a

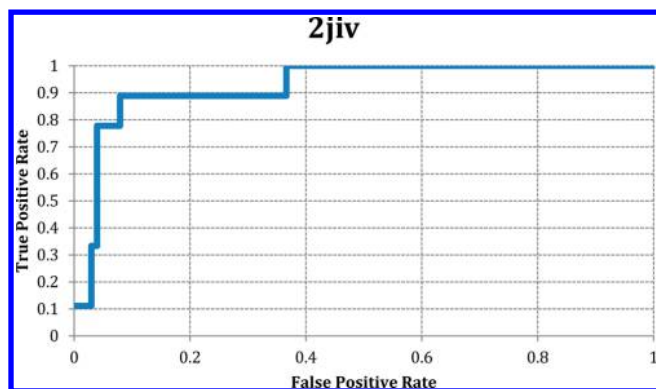


Figure 5. Receiver Operating Characteristic (ROC) of covalent docking virtual screening using 2jiv as the receptor.

more distant relative of cSrc and EGFR might make it a less ideal choice for this decoy set. For example, its binding pocket has more difference than the difference between the other two target families. The binding site RMSD (defined as heavy atoms within 5 Å of the ligand) between 3v6s and 2j5e is 1.83 Å, while the RMSD between 3lok and 2j5e is 1.62 Å.

3.3. SAR Study. In this study, we evaluated the performance of CovDock in attempting to rank two congeneric series of compounds, in order to establish if there was a correlation between calculated CovDock apparent binding affinity score and an experimental activity measurement. This is a challenging yet critically important issue in structure-based lead optimization. In covalent inhibitor design, there is additional complexity beyond that seen in a typical drug discovery project: the covalent inhibition process involves multiple steps in which the initial noncovalent binding of the prereactive species may or may not be the rate limiting step. Similarly the covalent bond formation may or may not be reversible. Thus, the experimental binding affinity is often not measured at equilibrium or cannot even be properly defined if the binding is irreversible, in significant contrast to the IC_{50} values routinely measured for a conventional noncovalent inhibitor design. The apparent IC_{50} values typically reported for covalent inhibitors are therefore typically measured at a specified time after the application of the potential inhibitor. The nature of this, in principle, nonequilibrium binding process must be taken into consideration when we compare the calculation to the experimental data. The preceding notwithstanding, we do here report the degree to which the CovDock apparent affinity score correlates with measurements of the experimental activity, with the expectation that even modest correlation may provide value to medicinal chemistry teams attempting to design novel covalent inhibitors. We should note though, the results presented for only two series cannot be considered a comprehensive study. However, the modest success in the following two cases perhaps suggests there may be some significant practical value in using CovDock to aid the lead optimization of covalent ligands

The first series in Figure 6 are 11 acrylamide inhibitors of cSrc kinase, which undergo a Michael reaction with the cysteine residue Cys345 in the binding pocket.²⁴ The correlation between calculated and experimental apparent binding activities is quite good with R-squared of 0.62. The docked poses of the strongest and weakest binders are shown below. These two compounds only differ in the far side of the warhead where one has a bromine atom ($RTln(IC_{50app}) = -9.7$ kcal/mol) and the

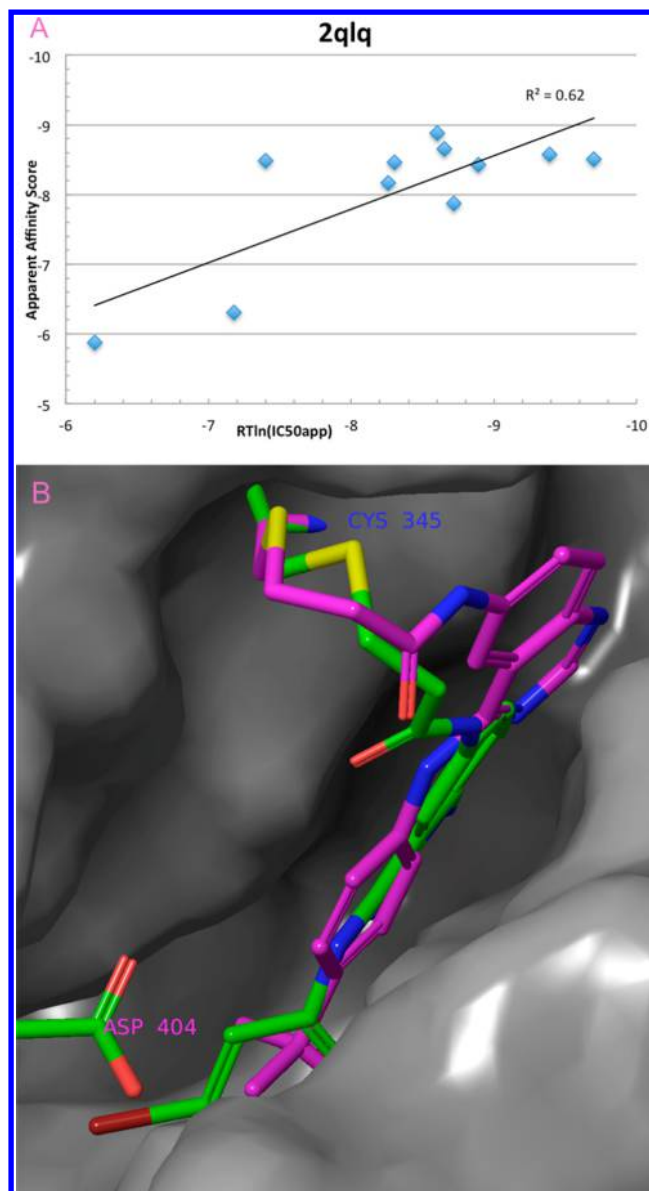


Figure 6. Apparent binding affinities of 11 acrylamide inhibitors of cSrc kinase. The docked poses of the strongest (green) and weakest (purple) binder are in panel B. The receptor is rendered as gray surface, except Cys345 and Asp404 which are shown in tube mode.

other has a *tert*-butyl group ($RTln(IC_{50app}) = -6.2$ kcal/mol). The docked poses show that the bottom of the binding pocket can fit the bromine but not the *tert*-butyl group, and thus the ligand with *tert*-butyl is pushed outside the pocket and receives a poor score.

The second series in Figure 7 are 26 peptidyl ketoamides against the HCV serine protease with a Nucleophilic addition to serine Ser139.²⁵ The binding pocket is shallow and solvent exposed with noncovalent interactions between the ligand and the receptor mainly taking the form of hydrogen bonds. Given the high degree of solvent exposure of the binding pocket, and the size and flexibility of the ligands in this set, we find it necessary to restrain the common core region to the ligands to obtain reasonable ligand binding modes. The R-squared of 0.32 is modest and may reflect unaccounted entropic contributions from the long flexible part of the ligands, or perhaps other undescribed kinetic contributions to the measured apparent

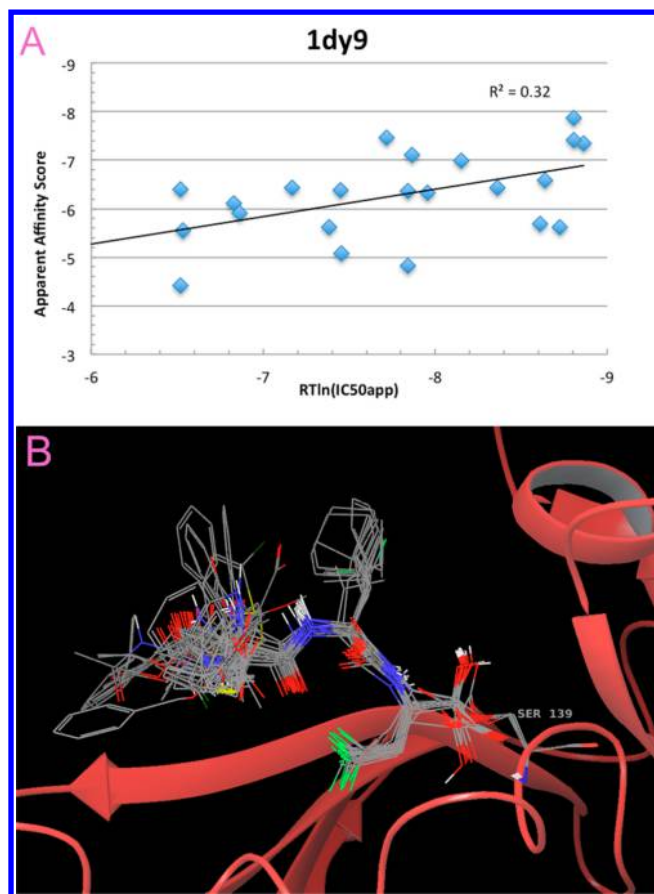


Figure 7. Apparent binding affinities of 26 peptidyl ketoamides against the HCV serine protease: Nucleophilic addition with core constraints.

IC50.²⁵ More advanced scoring technologies such as MMGBSA, free energy perturbation (FEP), or perhaps a Markov State Model based description of the covalent inhibitor binding process might provide better scoring performance for this kind of system, which we plan to investigate in future studies.

4. CONCLUSIONS

In this article, we here report a novel approach to the prediction of the binding modes of covalent inhibitors and further construct a physically justified, albeit empirical, scoring scheme, which appears to capture many of the salient features of effective covalent inhibition. This approach combines two of the most extensively validated programs in Schrödinger software suite, Glide and Prime, to extend their domain of applicability to this exciting application. Glide has been extensively validated to perform well in conventional ligand docking, but does not have the ability to optimize the receptor, nor can it handle the formation of a covalent bond between the ligand and the receptor. On the other hand, Prime has been extensively validated in the protein structure prediction, and its energy function is very accurate in ranking different conformations. The protocol presented here combines the strengths of both methods to produce a protocol more accurate than both either method by itself or by previously published methodologies designed specifically for this purpose. The ligand and receptor attachment residue are optimized simultaneously with OPLS force field and VSGB energy model, producing poses with realistic bond angles and bond

distances, which might be good starting geometries for further design work.

To our knowledge, the procedure for scoring of covalent inhibitors in this method is the first of its kind and has a firm albeit somewhat empirical physical foundation. Instead of directly modeling the energy of covalent bond formation as in Autodock4 and CovalentDock, our method takes into consideration the quality of the noncovalent interactions formed by the ligand at two steps along the reaction pathway and infers the quality of the covalent inhibitor from this information. The Prime optimization step further enables the use of standard force field parameters to define the covalent bond between the covalent inhibitor and protein, eliminating the need for a separate parametrization to be developed for each new reaction type. This approach leverages the well-validated Glide score function to descriptively model what is largely a kinetically driven process, by relying on the simplifying assumption that favorable covalent inhibitors must form favorable noncovalent interactions upon binding and maintain those favorable noncovalent interactions during the reaction process.

We have further validated the utility of this scoring function to provide enrichments in virtual screening applications and to facilitate approximate rank-ordering of members of congeneric series of compounds, all of which are assumed to undergo the same chemical reaction during the docking and have similar intrinsic reactivities. In some applications it may be desirable to screen mixtures of covalent and noncovalent inhibitors. The scoring approach constructed herein will apply a reward energy to the ligands that can form a covalent bond with the protein, so it may have some power in this regard, but accurate calculation of the contribution from the covalent bond, e.g., whether it is a reversible or irreversible reaction, what the reaction barrier is, etc., is beyond the scope of this work and may ultimately require a full quantum mechanical analysis. From a practical point of view, the warhead and the rest of the ligand are typically optimized in separate stages of a covalent inhibitor lead-optimization project, and thus the protocol reported herein may be of particular value to projects that have committed to a particular reactive warhead and are instead focused on the optimization of the remaining portion of the covalent inhibitor to improve apparent binding affinity to the target of interest.

■ ASSOCIATED CONTENT

■ Supporting Information

The list of PDB IDs and pose prediction results of the 76 complexes used in CovalentDock (Table S1), The chemical structures of 10 active compounds and 100 decoy compounds used in the virtual screening study (Table S2). This material is available free of charge via the Internet at <http://pubs.acs.org>.

■ AUTHOR INFORMATION

Corresponding Author

*E-mail: ed.harder@schrodinger.com.

Author Contributions

†K.Z. and K.W.B.: These authors contributed equally to this work.

Notes

The authors declare no competing financial interest.

ACKNOWLEDGMENTS

The authors would like to thank Dr. Shunqi Yan and Dr. Mee Shelley for helpful discussions.

REFERENCES

- (1) Singh, J.; Petter, R. C.; Baillie, T. A.; Whitty, A. The Resurgence of Covalent Drugs. *Nat. Rev. Drug Discovery* **2011**, *10*, 307–317.
- (2) Lin, C.; Kwong, A. D.; Perni, R. B. Discovery and Development of VX-950, a Novel, Covalent, and Reversible Inhibitor of Hepatitis C Virus NS3.4A Serine Protease. *Infect. Disord.: Drug Targets* **2006**, *6*, 3–16.
- (3) Njoroge, F. G.; Chen, K. X.; Shih, N.-Y.; Piwinski, J. J. Challenges in Modern Drug Discovery: a Case Study of Boceprevir, an HCV Protease Inhibitor for the Treatment of Hepatitis C Virus Infection. *Acc. Chem. Res.* **2008**, *41*, 50–59.
- (4) Honigberg, L. A.; Smith, A. M.; Sirisawad, M.; Verner, E.; Loury, D.; Chang, B.; Li, S.; Pan, Z.; Thamm, D. H.; Miller, R. A.; Buggy, J. J. The Bruton Tyrosine Kinase Inhibitor PCI-32765 Blocks B-Cell Activation and Is Efficacious in Models of Autoimmune Disease and B-Cell Malignancy. *Proc. Natl. Acad. Sci. U. S. A.* **2010**, *107*, 13075–13080.
- (5) Perni, R. B.; Chandorkar, G.; Cottrell, K. M.; Gates, C. A.; Lin, C.; Lin, K.; Luong, Y.-P.; Maxwell, J. P.; Murcko, M. A.; Pitlik, J.; Rao, G.; Schairer, W. C.; Van Drie, J.; Wei, Y. Inhibitors of Hepatitis C Virus NS3.4A Protease. Effect of P4 Capping Groups on Inhibitory Potency and Pharmacokinetics. *Bioorg. Med. Chem. Lett.* **2007**, *17*, 3406–3411.
- (6) Friesner, R. A.; Murphy, R. B.; Repasky, M. P.; Frye, L. L.; Greenwood, J. R.; Halgren, T. A.; Sanschagrin, P. C.; Mainz, D. T. Extra Precision Glide: Docking and Scoring Incorporating a Model of Hydrophobic Enclosure for Protein-Ligand Complexes. *J. Med. Chem.* **2006**, *49*, 6177–6196.
- (7) Goodsell, D. S.; Olson, A. J. Automated Docking of Substrates to Proteins by Simulated Annealing. *Proteins* **2009**, *8*, 195–202.
- (8) Jones, G.; Willett, P.; Glen, R. C.; Leach, A. R.; Taylor, R. Development and Validation of a Genetic Algorithm for Flexible Docking. *J. Mol. Biol.* **1997**, *267*, 727–748.
- (9) Morris, G. M.; Huey, R.; Lindstrom, W.; Sanner, M. F.; Belew, R. K.; Goodsell, D. S.; Olson, A. J. *Software News and Updates AutoDock4 and AutoDockTools4: Automated Docking with Selective Receptor Flexibility* **2009**, *30*, 2785–2791.
- (10) Ouyang, X.; Zhou, S.; Su, C. T. T.; Ge, Z.; Li, R.; Kwok, C. K. CovalentDock: Automated Covalent Docking with Parameterized Covalent Linkage Energy Estimation and Molecular Geometry Constraints. *J. Comput. Chem.* **2013**, *34*, 326–336.
- (11) Friesner, R. A.; Banks, J. L.; Murphy, R. B.; Halgren, T. A.; Klicic, J. J.; Mainz, D. T.; Repasky, M. P.; Knoll, E. H.; Shelley, M.; Perry, J. K.; Shaw, D. E.; Francis, P.; Shenkin, P. S. Glide: a New Approach for Rapid, Accurate Docking and Scoring. 1. Method and Assessment of Docking Accuracy. *J. Med. Chem.* **2004**, *47*, 1739–1749.
- (12) Halgren, T. A.; Murphy, R. B.; Friesner, R. A.; Beard, H. S.; Frye, L. L.; Pollard, W. T.; Banks, J. L. Glide: a New Approach for Rapid, Accurate Docking and Scoring. 2. Enrichment Factors in Database Screening. *J. Med. Chem.* **2004**, *47*, 1750–1759.
- (13) Jacobson, M. P.; Pincus, D. L.; Rapp, C. S.; Day, T. J. F.; Honig, B.; Shaw, D. E.; Friesner, R. A. A Hierarchical Approach to All-Atom Protein Loop Prediction. *Proteins* **2004**, *55*, 351–367.
- (14) Jacobson, M. P.; Friesner, R. A.; Xiang, Z.; Honig, B. On the Role of the Crystal Environment in Determining Protein Side-Chain Conformations. *J. Mol. Biol.* **2002**, *320*, 597–608.
- (15) Zhu, K.; Pincus, D. L.; Zhao, S.; Friesner, R. A. Long Loop Prediction Using the Protein Local Optimization Program. *Proteins* **2006**, *65*, 438–452.
- (16) Zhu, K.; Shirts, M. R.; Friesner, R. A. Improved Methods for Side Chain and Loop Predictions via the Protein Local Optimization Program: Variable Dielectric Model for Implicitly Improving the Treatment of Polarization Effects. *J. Chem. Theory Comput.* **2007**, *3*, 2108–2119.
- (17) Zhao, S.; Zhu, K.; Li, J.; Friesner, R. A. Progress in Super Long Loop Prediction. *Proteins* **2011**, *79*, 2920–2935.
- (18) Li, J.; Abel, R.; Zhu, K.; Cao, Y.; Zhao, S.; Friesner, R. A. The VSGB 2.0 Model: a Next Generation Energy Model for High Resolution Protein Structure Modeling. *Proteins* **2011**, *79*, 2794–2812.
- (19) Watts, K. S.; Dalal, P.; Murphy, R. B.; Sherman, W.; Friesner, R. A.; Shelley, J. C. ConfGen: a Conformational Search Method for Efficient Generation of Bioactive Conformers. *J. Chem. Inf. Model.* **2010**, *50*, 534–546.
- (20) Sastry, G. M.; Adzhigirey, M.; Day, T.; Annabhimoju, R.; Sherman, W. Protein and Ligand Preparation: Parameters, Protocols, and Influence on Virtual Screening Enrichments. *J. Comput.-Aided. Mol. Des.* **2013**, *27*, 221–234.
- (21) Schrodinger, Inc.: Maestro v9.5, 2013.
- (22) Shelley, J. C.; Cholleti, A.; Frye, L. L.; Greenwood, J. R.; Timlin, M. R.; Uchimaya, M. Epik: a Software Program for pK(a) Prediction and Protonation State Generation for Drug-Like Molecules. *J. Comput.-Aided. Mol. Des.* **2007**, *21*, 681–691.
- (23) Greenwood, J. R.; Calkins, D.; Sullivan, A. P.; Shelley, J. C. Towards the Comprehensive, Rapid, and Accurate Prediction of the Favorable Tautomeric States of Drug-Like Molecules in Aqueous Solution. *J. Comput.-Aided. Mol. Des.* **2010**, *24*, 591–604.
- (24) Blair, J. A.; Rauh, D.; Kung, C.; Yun, C.-H.; Fan, Q.-W.; Rode, H.; Zhang, C.; Eck, M. J.; Weiss, W. A.; Shokat, K. M. Structure-Guided Development of Affinity Probes for Tyrosine Kinases Using Chemical Genetics. *Nat. Chem. Biol.* **2007**, *3*, 229–238.
- (25) Colarusso, S.; Gerlach, B.; Koch, U.; Muraglia, E.; Conte, I.; Stansfield, I.; Matassa, V. G.; Narjes, F. Evolution, Synthesis and SAR of Tripeptide Alpha-Ketoacid Inhibitors of the Hepatitis C Virus NS3/NS4A Serine Protease. *Bioorg. Med. Chem. Lett.* **2002**, *12*, 705–708.